Circulation

ORIGINAL RESEARCH ARTICLE

Novel Desmin Mutation p.Glu401Asp Impairs Filament Formation, Disrupts Cell Membrane Integrity, and Causes Severe Arrhythmogenic Left Ventricular Cardiomyopathy/Dysplasia

Editorial, see p 1611

Francisco José Bermúdez-Jiménez, MD*
Víctor Carriel, MSc, MBiol, PhD*
Andreas Brodehl, MSc, PhD
Miguel Alaminos, MD, PhD
Antonio Campos, MD, PhD
Ilona Schirmer, MSc
Hendrik Milting, MSc, PhD
Beatriz Álvarez Abril, MD
Miguel Álvarez, MD, PhD
Silvia López-Fernández, MD
Diego García-Giustiniani, MD
Lorenzo Monserrat, MD, PhD
Luis Tercedor, MD
Juan Jiménez-Jáimez, MD, PhD

BACKGROUND: Desmin (*DES*) mutations cause severe skeletal and cardiac muscle disease with heterogeneous phenotypes. Recently, *DES* mutations were described in patients with inherited arrhythmogenic right ventricular cardiomyopathy/dysplasia, although their cellular and molecular pathomechanisms are not precisely known. Our aim is to describe clinically and functionally the novel *DES*-p.Glu401Asp mutation as a cause of inherited left ventricular arrhythmogenic cardiomyopathy/dysplasia.

METHODS: We identified the novel *DES* mutation p.Glu401Asp in a large Spanish family with inherited left ventricular arrhythmogenic cardiomyopathy/dysplasia and a high incidence of adverse cardiac events. A full clinical evaluation was performed on all mutation carriers and noncarriers to establish clinical and genetic cosegregation. In addition, desmin, and intercalar disc–related proteins expression were histologically analyzed in explanted cardiac tissue affected by the *DES* mutation. Furthermore, mesenchymal stem cells were isolated and cultured from 2 family members with the *DES* mutation (1 with mild and 1 with severe symptomatology) and a member without the mutation (control) and differentiated ex vivo to cardiomyocytes. Then, important genes related to cardiac differentiation and function were analyzed by real-time quantitative polymerase chain reaction. Finally, the p.Glu401Asp mutated *DES* gene was transfected into cell lines and analyzed by confocal microscopy.

RESULTS: Of the 66 family members screened for the *DES*-p.Glu401Asp mutation, 23 of them were positive, 6 were obligate carriers, and 2 were likely carriers. One hundred percent of genotype-positive patients presented data consistent with inherited arrhythmogenic cardiomyopathy/dysplasia phenotype with variable disease severity expression, high-incidence of sudden cardiac death, and absence of skeletal myopathy or conduction system disorders. Immunohistochemistry was compatible with inherited arrhythmogenic cardiomyopathy/dysplasia, and the functional study showed an abnormal growth pattern and cellular adhesion, reduced desmin RNA expression, and some other membrane proteins, as well, and desmin aggregates in transfected cells expressing the mutant desmin.

CONCLUSIONS: The *DES*-p.Glu401Asp mutation causes predominant inherited left ventricular arrhythmogenic cardiomyopathy/dysplasia with a high incidence of adverse clinical events in the absence of skeletal myopathy or conduction system disorders. The pathogenic mechanism probably corresponds to an alteration in desmin dimer and oligomer assembly and its connection with membrane proteins within the intercalated disc.

*Drs Bermúdez-Jiménez and Carriel contributed equally.

Key Words: arrhythmogenic right ventricular dysplasia ■ desmin ■ mutation ■ myopathy, myofibrillar, desmin-related ■ ventricular fibrillation

Sources of Funding, see page 1608

http://circ.ahajournals.org

Clinical Perspective

What Is New?

- Previously, *DES* mutations have frequently been related to skeletal myopathy and cardiac involvement, mainly as dilated or restrictive cardiomyopathy with atrioventricular conduction disorders.
- For the first time, we describe the largest arrhythmogenic right ventricular cardiomyopathy/dysplasia family to date with a single *DES* mutation with a phenotype of left dominant arrhythmogenic dysplasia in the absence of skeletal myopathy symptoms and atrioventricular conduction disorders, supported by strong clinical and functional data.
- New insights for further investigations are proposed: a failed connection of desmin with membrane proteins disrupting cell–cell adhesion and differences in RNA expression within *DES* mutation carriers of different genes associated with cardiomyopathies/channelopathies.

What Are the Clinical Implications?

- Patients presenting a cardiomyopathy characterized by mild left ventricular systolic dysfunction and dilation, fibrosis, ventricular arrhythmias, and a family history of sudden death, *DES* mutations should be suspected.
- These patients should undergo genetic testing, cardiac magnetic resonance to assess myocardial fibrosis, and Holter monitoring looking for ventricular arrhythmias.
- Additional research is necessary to elucidate the mechanisms linking *DES* mutations and nondesmosomal mutations (*FLNC*, *LMNA*) to this phenotype, to assess late gadolinium enhancement as a risk factor, and to determine a better risk stratification to improve survival in carriers with myocardial fibrosis and left ventricular systolic function relatively well preserved.

Arrhythmogenic right ventricular cardiomyopathy/dysplasia (ARVC/D) is an inherited disorder of genetic origin that causes malignant ventricular arrhythmias leading to sudden cardiac death (SCD).[1–4] Inherited ARVC/D (iARVC/D) is one of the most prevalent causes of SCD in young people, especially in athletes.[5] Left ventricular (LV) involvement is common and appears to imply a poorer prognosis. Mutations in genes encoding for desmosomal proteins (plakophilin-2 [*PKP2*], desmoplakin [*DSP*], desmoglein-2 [*DSG2*], desmocollin-2 [*DSC2*], and plakoglobin [*JUP*]) play a key role in the pathogenesis of this disease.[6–10] With the increasing use of the next-generation sequencing techniques in cardiovascular genetics, nondesmosomal and ion channels gene mutations[11] have also been associated with iARVC/D. Two prominent examples are the mutations p.S358L in *TMEM43* and p.Arg14del in *PLN*,[12] encoding the transmembrane protein Luma localized in the nuclear membrane[13,14] and a regulator of the sarcoplasmic reticulum Ca^{2+}-(SERCA2a) pump in cardiac muscle, respectively.

Some cytoskeletal proteins, such as filamin C[15] or desmin, are closely related to the development of cardiomyopathy. Desmin, encoded by the gene *DES*, is a structural intermediate filament present in the cytoskeleton of the leiomyocytes, rhabdomyocytes, and cardiomyocytes, and it is associated with different cellular structures, such as desmosomes, Z-bands, costameres, mitochondria, and the nuclei. Its function is related to the maintenance of the structural integrity of the cardiomyocyte.[16] More than 70% of the described pathogenic *DES* mutations exhibit cardiac involvement and can be associated with any form of cardiomyopathy, the most common being dilated cardiomyopathy, followed by restrictive, hypertrophic, ARVC/D, and their combinations.[17] It usually presents specific conduction system disturbance and, in addition, evidence of skeletal myopathy. The molecular pathogenic mechanisms causing the ARVC/D-related *DES* mutation phenotype are unknown, and preexisting data in this regard are rare.

In this study, we demonstrate the pathogenicity of the novel *DES* mutation p.Glu401Asp in a large family with an inherited LV dominant arrhythmogenic cardiomyopathy/dysplasia and a high incidence of adverse clinical events, such as SCD, major heart failure, and ventricular arrhythmia. We also identify the cellular, histological, and molecular mechanisms leading to the appearance of the iARVC/D phenotype.

METHODS

The data, analytic methods, and study materials will not be made available to other researchers for purposes of reproducing the results or replicating the procedure.

Study Population and Clinical Variables

The study population included all available members of a large Spanish family of white origin, composed of 83 individuals spread over 6 generations. Sixty-six family members were available for evaluation (51.6% male; mean age, 43.3±19.3 years old). The study protocol was approved by the local ethics committee (University of Granada) on March 2016. All patients included in the study signed an informed consent form.

Clinical Study

All subjects underwent an initial clinical evaluation that included a clinical history with particular emphasis on the presence of adverse events such as death, heart failure death, SCD, atrioventricular block, sustained ventricular arrhythmia, syncope, heart transplantation, or cardiac device implantation. In addition, all subjects underwent a 12-lead ECG, a

transthoracic echocardiogram, a creatine phosphokinase blood test, and a neuromuscular examination to investigate involvement of the skeletal muscle. The mutation carriers underwent 24 hours of ambulatory ECG monitoring (Holter) and a cardiac magnetic resonance (CMR) imaging. The CMR imaging was performed in all participants who accepted the procedure and had no contraindications (cardiac device implant and claustrophobia). The ECG data were analyzed to obtain the PR, QRS, and QT intervals in milliseconds, and data on voltage, conduction disturbance, and the presence of pathological Q waves. In the 24-hour ambulatory ECG, we analyzed the presence of nonsustained ventricular tachycardia, atrioventricular block, and ventricular ectopy morphology and density. The evaluation of LV diameter and function was performed according to current guidelines,[18] including LV end-diastolic and end-systolic diameter and volume, LV ejection fraction using the Simpson biplane method, right ventricular outflow and inflow tract diameter, and right ventricular systolic function, as well. Diagnosis of the index patient was based on modified Arrhythmogenic Right Ventricular Cardiomyopathy/Dysplasia Task Force criteria.[19] All clinical tests were interpreted by cardiologists specialized in advanced cardiac imaging and electrophysiology. Data collection was limited by the lack of both electro- and echocardiographic information on deceased and precardiac transplant subjects in the corresponding cases. Furthermore, the statistical analysis did not include clinical data or complementary tests of children <13 years of age.

Genetic Analysis

After obtaining the peripheral blood of the index patient (IV.31 on Figure 1), the genetic analysis was performed by using a next-generation sequencing gene panel containing 149 genes (Figure I in the online-only Data Supplement). This study included an analysis of all coding exons and intron flanking regions of a personalized panel of genes, which had been previously associated with or are regarded as candidates for the development of hereditary cardiovascular diseases. Sample preparation was performed using the Agilent SureSelect Target Enrichment Kit based on the paired-end multiplexed sequencing method according to the manufacturer's instructions. Low-coverage regions of the relevant genes were resequenced using the Sanger method. Bioinformatic analysis was performed through an in-house–developed pipeline that included software such as NovoAlign, SAMtools, and BCFtools. Information such as frequency in different populations (from sources including exome variant server, 1K genomes, and the Single Nucleotide Polymorphism Database), and various bioinformatic predictions, as well, was added. Pathogenicity of the identified variants was classified according to current guidelines of the American College of Medical Genetics and Genomics.[20] Following mutation *DES*-p.Glu401Asp identification in the index patient, genetic and clinical cascade screening was performed on all available family members.

Histological Analysis

Cardiac tissue from patient III.21 (Figure 1) carrying *DES*-p.Glu401Asp and subjected to heart transplantation was used for histological analysis. In addition, normal healthy cardiac tissue obtained from a patient without the mutation was used as control. The tissues were fixed for 24 hours in 10% neutral buffered formaldehyde, washed, dehydrated in ascending concentrations of ethanol, cleared in xylene, and embedded in paraffin using a conventional protocol.[21] Five-micrometer histological sections were dewaxed and stained with hematoxylin-eosin for morphological evaluation. Stromal collagen fibers were histochemically evaluated by picrosirius staining as described elsewhere.[22] To evaluate myofibril organization in the cardiomyocytes, tissue sections were histochemically stained according to the Heidenhain iron hematoxylin method as previously described.[23] The histomorphological pattern of the desmin intermediate filament was evaluated by indirect immunohistochemistry. Desmosomes and intercellular gap junctions localized at the intercalated discs were identified by immunohistochemical staining of desmoplakin, plakoglobin, and connexin-43, respectively. Immunohistochemistry was prepared as previously described[22–24] using positive and negative technical controls. All procedures were performed simultaneously under the same conditions to ensure reproducibility of the results. Technical information about the used antibodies is summarized in Table I in the online-only Data Supplement.

Stem Cell Culture and Cardiomyocyte Differentiation

To evaluate the impact of *DES* mutation on cell function, adipose-derived mesenchymal stem cells (ADMSCs) were isolated from subcutaneous adipose biopsies obtained from 3 members of the family evaluated in this study: a healthy non-*DES* mutation carrier (healthy control) and 2 mutation carriers, 1 with mild symptomatology and 1 with a severe clinical condition, were included. The biopsies were mechanically fragmented into small pieces and then digested for 8 hours in a 2 mg/mL solution of *Clostridium histolyticum* type I collagenase (Gibco BRL Life Technologies) as previously described.[21] The ADMSCs were harvested by centrifugation and cultured in a basal medium consisting of DMEM supplemented with 10% FBS and antibiotics-antimycotics (Sigma-Aldrich). After obtaining a subconfluent cell culture, the ADMSCs were differentiated ex vivo into the cardiomyocyte lineage, using the Gibco Cardiomyocyte Differentiation Kit (A29212-01, Thermo Fisher Scientific), for 14 days according to the manufacturer's instructions. The growth pattern and differentiation process of these cells were continuously monitored by phase-contrast microscopy. The human cardiomyocyte phenotype was confirmed using a commercially available Human Cardiomyocyte Immunocytochemistry Kit (A25973, Thermo Fisher Scientific).

Real-Time Quantitative Polymerase Chain Reaction Analyses

Total RNA was extracted from each cell type (differentiated and nondifferentiated cell cultures from each of the 3 family members studied) using a Qiagen RNeasy Mini Kit system (Qiagen). Then, cDNA was synthetized from total RNA with an iScript Advanced cDNA Synthesis Kit (Bio-Rad Laboratories) using 1 µg of each RNA. Expression quantification of a set of genes with important roles in cardiac differentiation and function was analyzed using real-time quantitative polymerase chain reaction (PCR). Thus,

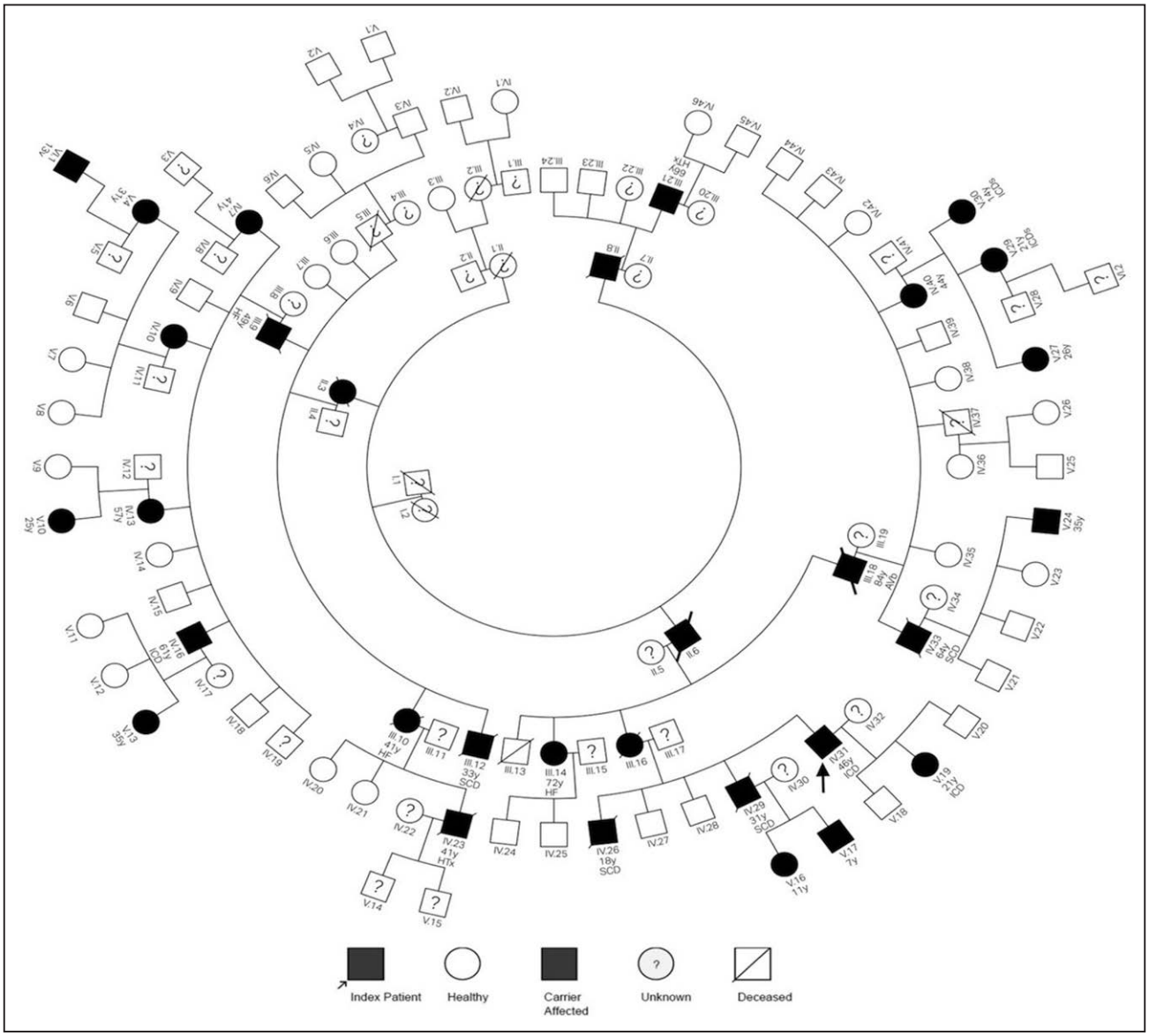

Figure 1. Full pedigree with a large number of clinical events.
Squares and circles represent males and females, respectively. Mutation carriers are marked in black, noncarriers in white, and those not studied in gray. Deceased are indicated by a slash. HF indicates heart failure; HTx, heart transplant; ICD, implantable cardioverter defibrillator; ICDs, subcutaneous implantable cardioverter defibrillator; SCD, sudden cardiac death; and VT, ventricular tachycardia.

a 96-well plate containing oligonucleotides for the genes and controls selected was designed as a PrimePCR custom assay. The selection of these genes was based on 2 previously described gene expression panels for cardiac diseases: Cardiac Arrhythmia Next-Generation Sequencing Multi-Gene Panel and Bio-Rad Arrhythmias Cardiac H96 Panel. For each PCR reaction, 2 µL of cDNA, 8 µL of H_2O, and 10 µL of SsoAdvanced Universal SYBR Green Supermix were added, and a PCR protocol consisting of 40 amplification cycles with an annealing temperature of 60°C was applied using a Bio-Rad CFX Connect-96 instrument. Results were corrected according to the efficiency of the reverse transcription reaction and normalized to the *GAPDH* housekeeping gene expression using Bio-Rad CFX Manager 3.1 software. Each sample was analyzed in triplicate (n=18). Relative gene expression was calculated for each gene using the ΔΔCq value (CFX Manager 3.1 software, Bio-Rad) by comparing each differentiated cell culture with its nondifferentiated control samples. By using this approach, we obtained the fold-change expression increase or decrease of every gene in the 3 sample types analyzed as average differentiated cell expression divided by average nondifferentiated cell expression. The fold-changes obtained for the unmutated control cells were considered as the basal levels of normal cells for each gene, whereas the fold-changes obtained for both samples were compared with basal levels. Genes showing an increase or decrease of at least 2-fold, in comparison with basal levels, were selected.

Plasmids, Cell Culture, and Confocal Microscopy

The expression plasmid pmRuby-N1-Desmin has been previously described.[25] This construct encodes a C-terminal fusion protein of human desmin and the fluorescence protein mRuby that was used for direct fluorescence microscopy. The mutations p.Glu401Asp and p.Glu401Lys were introduced using the QuickChange Lightning Site-Directed Mutagenesis Kit (210518, Agilent Technologies). The mutation insertions were verified by Sanger sequencing (Macrogen). SW13 cells were grown with ≈70% confluency on cover slips in DMEM (Gibco; 4.5 g/L glucose, 10% FBS, supplemented with penicillin/streptomycin). These cells were used because they do not express endogenous desmin or any other cytoplasmic intermediate filament protein. The cells were transiently transfected with Lipofectamine 2000 (Thermo Fisher Scientific) according to the manufacturer's instructions. Twenty-four hours after transfection, the cells were washed several times for 5 minutes with PBS and fixed for 5 minutes with Roti Histofix (Carl Roth). They were then extensively washed in PBS and permeabilized with Triton X-100 (0.1% in PBS). F-actin was stained with fluorescein isothiocyanate–conjugated phalloidin (Sigma-Aldrich) 50 µg/mL for 40 minutes at room temperature according to the manufacturer's instructions. The cells were embedded in Mowiol 4 to 88 (Carl Roth). Confocal laser scanning microscopy was performed with the TCS SP8 system (Leica Microsystems) equipped with a HC PL API C52 (63×/1.30) glycerin objective, hybrid detectors, and Application Suite X software. The fluorescence molecules mRuby and fluorescein isothiocyanate were sequentially excited. Each cell culture experiment was performed in triplicate.

Statistical Analysis

Statistical calculations were performed using SPSS Statistics (version 20, IBM Corp). Clinical characteristics were compared using χ^2 or Fisher exact test for categorical variables and Student *t* test or Mann-Whitney *U* test for continuous variables. All categorical data were reported as frequencies and percentages, and continuous variables were expressed as mean value±SD for each measurement. A *P* value of <0.05 was considered to be statistically significant. Survival analysis was estimated by using the Kaplan-Meier method.

RESULTS

Genetic Analysis

The genetic analysis of the index patient (IV:31, Figure 1) revealed the heterozygous missense mutation in *DES* (NM_001927.3:c.1203G>C; NP_01918.3:p.Glu401Asp or p.E401D). This variant had not been previously described in any publication or in public databases, such as the Human Gene Mutation Database,[26] the Single Nucleotide Polymorphism Database,[27] NHLBI GO Exome Sequencing Project,[28] and ClinVar,[29] or in the Exome Aggregation Consortium (ExAC) database[30] (as of 31/03/2017). Amino acid residue E401 belongs to the fourth α-helix (coil 2B, amino acids 296–412) of the α-helical central rod domain (109–412), a region that is essential for desmin filament assembly. The in silico prediction indicated that p.Glu401Asp substitution NC_000002.11:g220286241G>C affects a highly conserved amino acid residue among different species (Figure II in the online-only Data Supplement).

Clinical Analysis

The index patient, a 46-year-old man (IV:31, Figure 1), was referred for examination because of a family history of SCD of 2 brothers aged 31 (IV:29) and 18 (IV:26). Postmortem examination of one of these brothers (IV.29) revealed epicardial and midwall fibrosis from the inferior LV wall to the septum and lateral wall. The right ventricle looked macroscopically normal, and there was no evidence of coronary artery disease. Histological examination showed focal areas of subendocardial fibrosis in the free wall of the right ventricle. In the left ventricle, subepicardial and midwall fat and fibrous tissue were confirmed, presenting widespread spaces admixed with degenerative myocytes. Myocardial inflammation was absent. In addition, there were no pathological findings suggestive of skeletal myopathy such a myofiber necrosis or myofiber atrophy. In summary, the postmortem study strongly suggested dominant inherited arrhythmogenic left ventricular cardiomyopathy/dysplasia.[31] The patient presented New York Heart Association functional class II symptoms with generalized T-wave inversion in all precordial leads and biventricular dilation and severely depressed biventricular ejection fraction, as well. These data were confirmed by CMR, which also showed late gadolinium enhancement at the subepicardial LV level. The 24-hour Holter study showed >500 of premature ventricular complexes with both left and right bundle-branch block morphologies. Finally, he was diagnosed to have inherited arrhythmogenic cardiomyopathy/dysplasia with biventricular involvement and received a cardiac defibrillator implantation for primary prevention of SCD.

In total, 66 family members were genetically sequenced for *DES*-p.Glu401Asp, of whom 23 presented the mutation; an additional 6 subjects were obligate carriers (deceased before sequencing), and another 2 nongenotyped cases, with, however, a previous SCD event, were considered probable carriers, corresponding to a total of 31 affected family members. Cosegregation analysis was performed to correlate genotype and phenotype, clearly confirming the pathogenic impact of this specific *DES* mutation. Evidence of primary myocardial disease was present in 100% of carriers, with variable clinical expression, whereas noncarriers showed no traces of nonischemic cardiomyopathy (Table II in the online-only Data Supplement). One noncarrier patient presented LV systolic dysfunction and atrioventricular block of ischemic origin.

Table. Clinical and Genetic Data in Subjects Carrying *DES* Mutation

Case*	Age at Dx, y	Sex	Gen Status	Symptoms	Major Events	CK, mg/dL	ε-Wave	T-Wave Inversion	Low Voltage†
II:3	n/a	F	OC	n/a	n/a	n/a	n/a	n/a	n/a
II:6	n/a	M	OC	n/a	n/a	n/a	n/a	n/a	n/a
II:8	41	M	OC	n/a	aHF	n/a	n/a	n/a	n/a
III:9	49	M	OC	n/a	aHF	n/a	n/a	n/a	n/a
III:10	41	F	OC	n/a	aHF	n/a	n/a	n/a	n/a
III:12	33	M	PC	n/a		n/a	n/a	n/a	n/a
III:14	72	F	C	Asymptomatic	aHF	53	No	V_1–V_6inferior	Yes
III:16	n/a	F	OC	n/a		n/a	n/a	n/a	n/a
III:18	84	M	C	Palpitations	AVb	n/a	No	No	No
III:21	66	M	C	Dyspnea	AHF; HTx	n/a	No	V_1–V_6inferior	No
IV:7	41	F	C	Asymptomatic		93	No	No	No
IV:10	55	F	C	Asymptomatic		103	No	No	Yes
IV:13	57	F	C	Asymptomatic		88	No	V_4–V_6inferior	Yes
IV:16	61	M	C	Dyspnea	aHF	95	No	No	No
IV:23	41	M	C	Syncope	aHF; HTx	76	No	V_1–V_2	No
IV:26	18	M	PC	n/a	SD	n/a	n/a	n/a	n/a
IV:29	31	M	C	Palpitations	SD	n/a	n/a	n/a	n/a
IV:31‖	47	M	C	Dyspnea	aHF	59	No	V_1–V_6inferior	Yes
IV:33	63	M	C	Asymptomatic	SD	112	No	No	No
IV:40	44	F	C	Asymptomatic		110	No	No	Yes
V:4	31	F	C	Asymptomatic		65	No	V_1–V_5inferior	Yes
V:13	34	F	C	Asymptomatic		41	No	V_4–V_6inferior	Yes
V:16	11	F	C	Asymptomatic		67	No	V_1–V_4	No
V:17	7	M	C	Asymptomatic		180	No	No	No
V:19	21	F	C	Palpitations	aHF	86	No	V_1–V_6inferior	Yes
V:10	25	F	C	Asymptomatic		105	Yes	V_5–V_6I-aVL	Yes
V:24	35	M	C	Palpitations		150	No	V_2–V_6inferior	Yes
V:27	26	F	C	Asymptomatic		55	No	V_1–V_6inferior	Yes
V:29	21	F	C	Asymptomatic		84	Yes	V_4–V_6inferior	No
V:30	14	F	C	Asymptomatic		59	No	V_4–V_6inferior	No
VI:1	13	M	C	Asymptomatic		103	No	V_1–V_4	Yes

(*Continued*)

Of the 23 carriers studied, 9 fulfilled the modified diagnostic criteria. Main clinical and genetic data of *DES* mutation carriers are summarized in the Table. The most common ECG finding was T-wave inversion in at least 3 consecutive ECG leads (14 cases) and generalized low voltage (12 cases). The ECG was abnormal in 97% of the carriers for whom it was available, mostly because of the presence of negative T waves in inferior (II, III, aVF) and anterolateral leads (V_2 through V_6) (Figure 2A). No change was detected in the PR interval, which was similar in both groups, although a wider QRS was identified in the carrier group (Table II in the online-only Data Supplement). Two of the 3 affected children (7, 11, and 13 years old) presented negative T wave beyond V_3. One of them (VI.1) showed low voltages in limb leads in the ECG and subepicardial late gadolinium enhacement in inferior wall in the CMR. The 24-hour Holter study revealed nonsustained ventricular tachycardias in 32% of carriers and high-density ventricular ectopy in 23% of them. There was only 1 case of atrioventricular block in an 84-year-old man. We found no evidence of skeletal myopathy, and creatine phosphokinase determination was normal in all mutation carriers.

The most characteristic finding of the cardiac structure and function studied by echocardiography and CMR was near-exclusive LV affection, with hypokinesia localized on the midapical inferolateral wall of the

Table. Continued

LV DD	LV EF	LV WMA	RV Affect.‡	LV LGE	Ventricular Arrhythmias	Criteria§M/m	Comments
n/a	n/a	n/a	n/a	n/a	n/a	0/1	
n/a	n/a	n/a	n/a	n/a	n/a	1/0 Possible	
n/a	n/a	n/a	n/a	n/a	n/a	1/0Possible	
n/a	n/a	n/a	n/a	n/a	n/a	1/0 Possible	
n/a	n/a	n/a	n/a	n/a	n/a	1/0Possible	Heart failure death
n/a	n/a	n/a	n/a	n/a	n/a	1/0Possible	
48	43	Yes	No	Yes	NSVT; 970 VE	1/2Definite	
n/a	n/a	n/a	n/a	n/a	n/a	1/0Possible	
50	55	Yes	No	n/a	n/a	0/1	PM
n/a	n/a	n/a	n/a	n/a	NSVT	2/1Definite	
42	55	No	No	Yes	1868 VE	0/1	
54	48	Yes	No	Yes	8455 VE	0/1	
46	55	Yes	No	n/a	5852 VE	0/2Possible	
60	30	Yes	Yes	Yes	4479 VE	1/1Borderline	CRT-D
70	30	Yes	Yes	n/a	SVT; 8045 VE	2/1Definite	Heart failure death
n/a	n/a	n/a	n/a	n/a	n/a	2/0Definite	Died during exercise
n/a	n/a	n/a	n/a	n/a	n/a	1/0Possible	Died at rest
61	30	Yes	Yes	Yes	SV; 1283 VE	4/0Definite	CRT-D, aSH
55	52	Yes	No	Yes	193 VE	0/1	Died at rest (64 y) VT
49	57	Yes	No	Yes	342 VE	1/0Possible	
50	54	Yes	No	Yes	421 VE	1/0Possible	
54	49	Yes	No	n/a	1392 VE	1/1Borderline	
47	65	No	No	n/a	74 VE	Not applicable	
41	65	No	No	n/a	0 VE	Not applicable	
48	37	Yes	Yes	Yes	5293 VE	3/1Definite	aSH, ICD
49	39	Yes	No	Yes	NSVT; 2866 VE	0/2Possible	
62	50	Yes	No	Yes	2318 VE	1/1Borderline	
52	40	Yes	Yes	No	3216 VE	1/2Definite	
52	43	Yes	No	No	NSVT	2/1Definite	ICDs
53	40	Yes	No	Yes	NSVT	2/1Definite	ICDs
58	51	No	No	Yes	3985 VE	Not applicable	

aHF indicates advanced heart failure; aSH, appropriate ICD shock; AVb, atrioventricular block; C, carrier; CK, plasma levels of creatine kinase; CRT-D, cardiac resynchronization therapy defibrillator; Dx, diagnosis; F, female; Gen status, genotype status; HTx, heart transplant; ICD, implantable cardioverter defibrillator; ICDs, subcutaneous cardioverter defibrillator; LGE, presence of late gadolinium enhancement on cardiac magnetic resonance images; LV, left ventricle; LVDD, left ventricular end diastolic diameter; LVEF, left ventricular ejection fraction; LVWMA, left ventricular wall motion abnormalities; M, male; M/m, major/minor; n/a, data not available; NSVT, nonsustained ventricular tachycardia; OC, obligate carrier of the mutation; PC, probable carrier of the mutation; PM, pacemaker; RV, right ventricular; SD, sudden death; SVT, sustained ventricular tachycardia; VE, ventricular ectopics in 24-hour Holter monitoring; and VT, ventricular tachycardia.

*Case lists individual identifications according to position in the pedigree.

†Low voltage indicates the low QRS voltage amplitude on limb leads.

‡RV affect. shows right ventricular affection (akinesia, dyskinesia, aneurysm, dilatation, and systolic dysfunction).

§Criteria (major/minor): diagnostic status according to Arrhythmogenic Right Ventricular Cardiomyopathy/Dysplasia Task Force criteria.

‖Index patient.

LV, mildly depressed LV ejection fraction (46±8.2%), and no ventricular dilation (51.52±5.87 mm, normal in terms of body surface in most cases). Right ventricular involvement was demonstrated only in 5 cases that presented concomitant moderate/severe LV ejection fraction impairment, suggesting a primary involvement of the LV and subsequent right ventricular affection. Furthermore, CMR revealed an extensive late gadolinium enhancement with a typical circumferential subepicardial pattern in most of the cases, and midapical lateral and inferolateral subepicardial distribution in the remaining patients (Figure 2B).

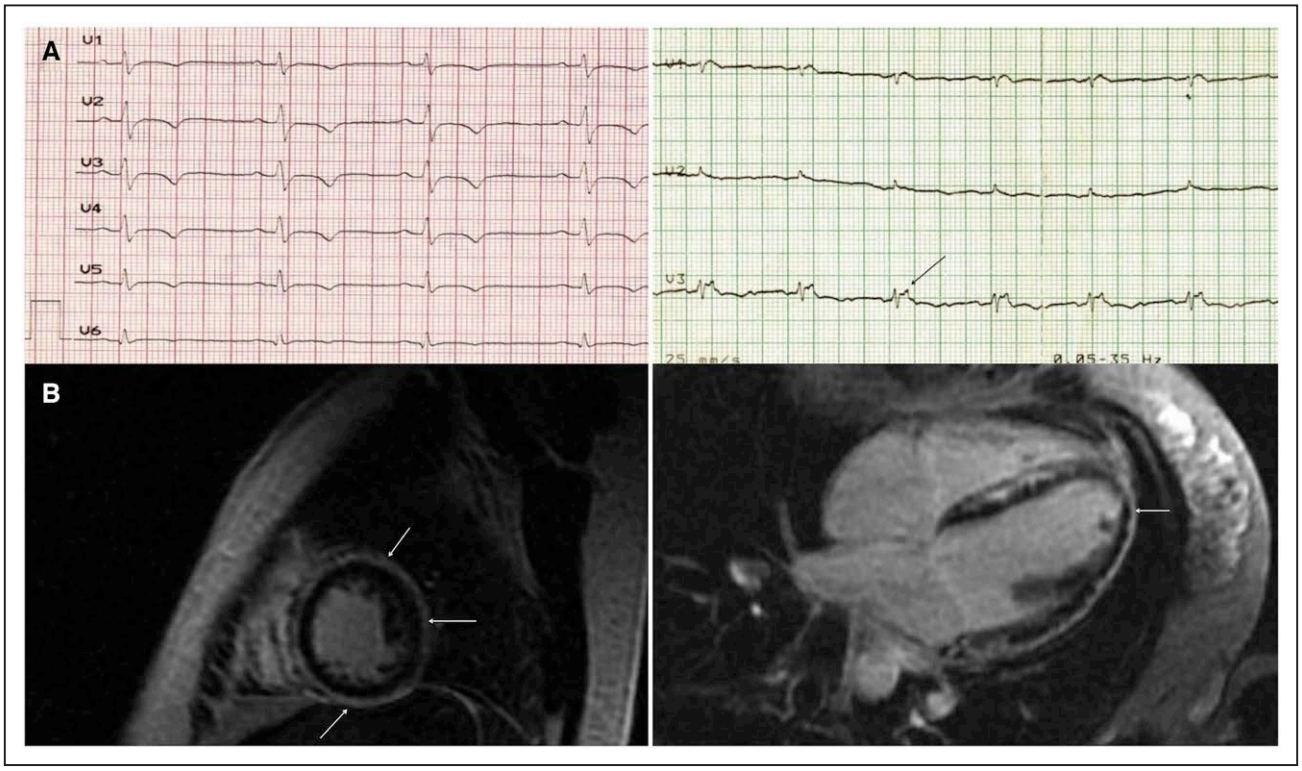

Figure 2. Clinical characteristics of *DES* mutation carriers.
A, ECG of 2 of the cases affected by mutation Glu401Asp. **Left,** The generalized inversion of the T wave, the lateral Q wave, and low voltage in body surface leads in proband's ECG (case IV.31). **Right,** The proband's mother's ECG (III.16) shows very low QRS voltage overall, with an ε-wave in all precordial leads (arrow). **B,** Imaging of left ventricular late gadolinium enhancement with subepicardial annular fibrosis (arrows) of patient V.30.

During familial screening, 15 of affected individuals were asymptomatic at diagnosis, 4 presented with palpitations, 3 with heart failure symptoms, and 1 with syncope. None showed myocarditis-like symptoms. It is noteworthy that patients with heart failure showed severe LV ejection fraction impairment at presentation (2 of them had a previous diagnosis of idiopathic dilated cardiomyopathy). A high incidence of cardiac events, mainly arrhythmic-related, was observed among carriers retrospectively and during follow-up (Table II in the online-only Data Supplement and Figure 3): 4 SCD (18, 31, 33, and 64 years old), 2 heart failure deaths (both at 41 years old), 1 atrioventricular block (84 years old), 2 heart transplantations (39 and 60 years old), 1 sustained monomorphic ventricular tachycardia (37 years old), and 5 implantable cardioverter defibrillators for primary prevention of SCD with 2 episodes of appropriate therapies on follow-up (21 and 47 years old). These findings support a high risk for malignant arrhythmias and SCD as first clinical manifestation.

Histological Analysis of Cardiac Tissue Affected by Desmin Mutation

Histological analysis of the heart from a desmin mutation carrier (III:21) showed major differences in comparison with the control heart. Picrosirius staining in the control tissue revealed that all cardiomyocytes showed their typical branched cylindrical shape, a single and centrally located nucleus, a highly dense and strongly stained sarcoplasm, and several intercalated discs between adjacent cells (Figure 4A). With regard to cardiac tissue affected by desmin mutation p.Glu401Asp, it was possible to recognize zones affected by typical degenerative changes and others with a more conserved myocardium. Degenerative findings were found associated with the subepicardial myocardium, where picrosirius staining revealed an increase of disorganized collagen fibers, the presence of infiltrating adipose tissue, and groups of cardiomyocytes with degenerative changes. However, these findings were not accompanied by an inflammatory reaction (Figure 4B). In the myocardial zones without degenerative changes, the tissue organization was preserved and comparable to the control. However, cell thickness was irregular, and an increased perinuclear space, accompanied by a relatively normal nucleus, was observed. Curiously, the sarcoplasm of these cells was weakly stained, less dense with less prominent intercalar discs than the control tissue (Figure 4). Heidenhain hematoxylin staining, which specifically stains myofibrils, confirmed the presence of fewer contractile myofibrils in the desmin mutation

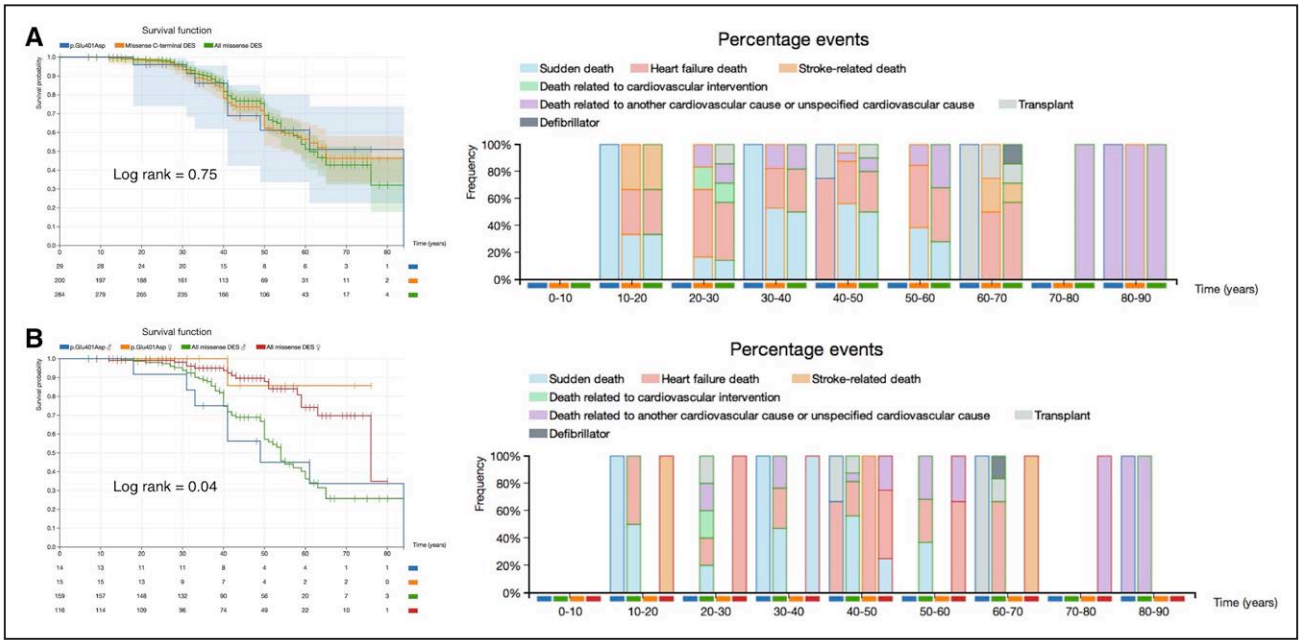

Figure 3. Event-free survival curves for major cardiac events in Glu401Asp *DES* mutation carriers.
A, The curve is similar to other missense *DES* mutations (data obtained from our genetic laboratory and from published literature, including data from 284 patients with *DES* mutations). **Right**, A breakdown of all cardiac events for different age ranges according to the presence of the Glu401Asp mutation, all C-terminal *DES* mutations, or all missense DES mutations. Note the high incidence of SCD at younger ages among patients with Glu401Asp mutation in comparison with patients with other *DES* mutations. **B,** A significant poorer prognosis is observed in males in comparison with females, as described for other *DES* missense mutations. Note the low incidence of major cardiac events in women carrying Glu401Asp until the age of 50, with no SCD cases. SCD indicates sudden cardiac death.

carrier's myocardium in comparison with the control. Myofibrils were less abundant, poorly organized, and less compacted, with spaces observed among them. Immunohistochemical analysis of desmin showed an intense and homogeneously distributed staining pattern in the sarcoplasm of both cardiac tissues, although it was more intense in the control intercalated discs. In addition, we did not observe any prominent desmin aggregates in the sarcoplasm of the cardiac tissue from this mutation carrier. After analyzing some important structural and functional proteins of cell–cell junctional complexes at the intercalated discs, desmoplakin, plakoglobin, and connexin-43 were observed to be positive in both cardiac tissues, thus confirming the presence of these junctional complexes. However, desmoplakin and plakoglobin were weakly stained in the myocardial tissue from the mutation carrier in comparison with the control. The connexin-43 intensity and pattern were comparable in control and affected tissue, as previously described with regard to another *DES* mutation, p.A120D[32] (Figure 4C).

ADMSC Differentiation and Gene Expression Analysis

Cell cultures established from different family members showed that all cell types were able to grow and proliferate ex vivo under standard culture conditions. Control cells isolated from the control family members without the *DES* mutation (healthy control) showed a typical mesenchymal morphology (elongated, spindle-shaped, flattened cells). As expected, confluent cells managed to fully cover the culture flask surface, which is typical of mesenchymal stem cells (Figure 5). In a similar manner, cells isolated from patients with the *DES* mutation showing mild symptomatology showed similar cell morphology and growth pattern to controls, although they tended to grow and proliferate more slowly. It is curious that cells from the affected *DES* mutation carrier patient (IV.31) grew much more slowly than the mild phenotype cell line and especially than the healthy control cell line. In addition, these cells presented a typical mesenchymal morphology, although their growth pattern was very different. In fact, they had difficulty adhering to the culture surface, resulting in a reticular pattern, with cells tending to adhere to one another rather than to the culture surface (Figure 5).

When ADMSCs were differentiated into cardiomyocytes, some cells could be observed to acquire a typical cardiomyocyte morphology, although the percentage of cells showing this phenotype was low. Differentiated cells were characterized by a large and polygonal cytoplasm with a thick, well-organized cytoskeleton (see representative images in Figure IIIA in the online-

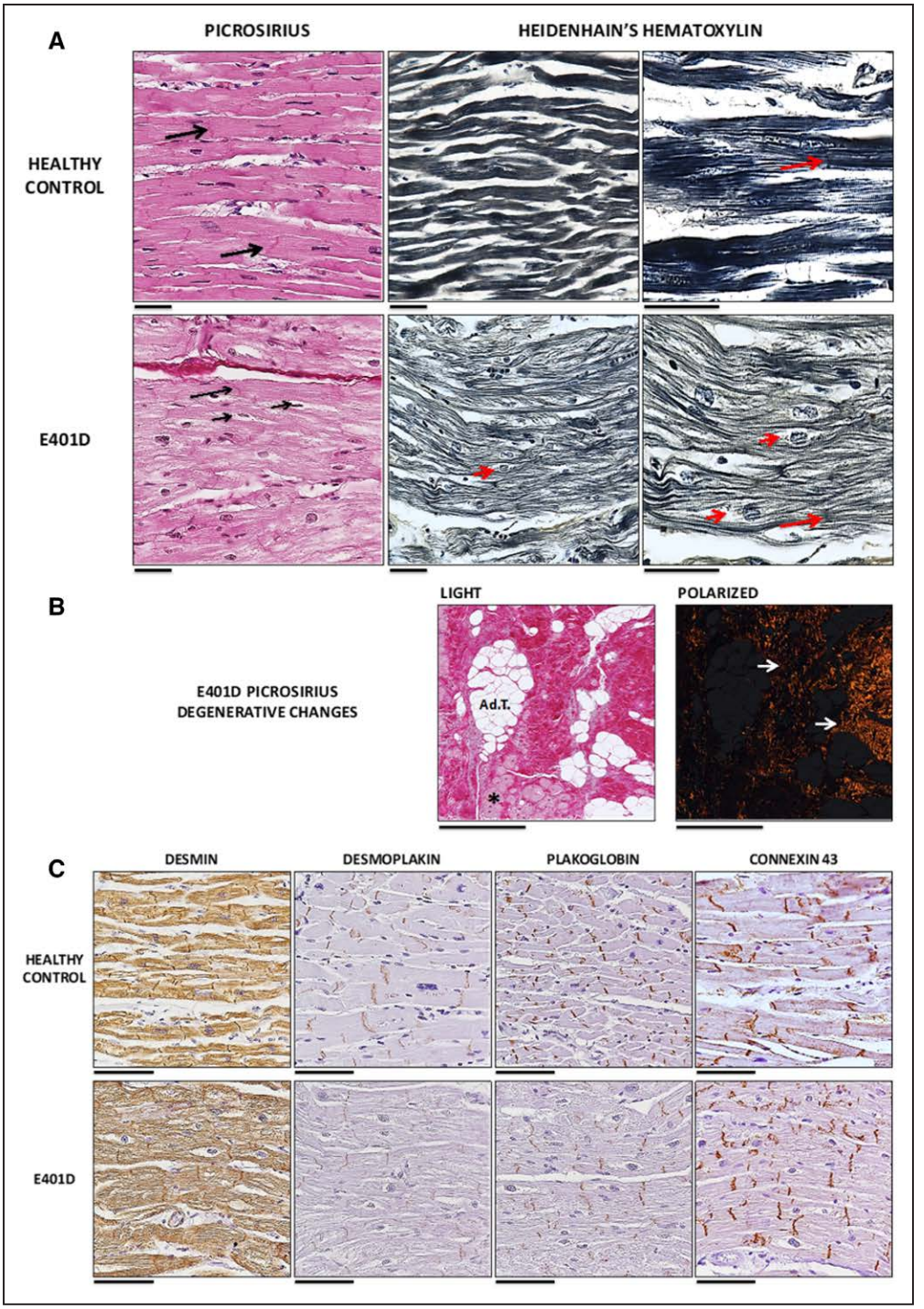

Figure 4. Histological analysis of cardiac tissue affected by desmin mutation.
A, Histochemical analyses of control heart (healthy control) and desmin-mutated cardiac tissue (Glu401Asp) by picrosirius and Heidenhain hematoxylin staining. Large black and red arrows show the intercalary disc, whereas the short black and red arrows show the perinuclear space in Glu401Asp. **B,** Representative images of the fibrotic reaction (arrows), adipose tissue replacement (Ad.T.) and cardiomyocyte degeneration changes (asterisk) in Glu401Asp are shown with picrosirius staining at light and polarized microscopy. **C,** Immunohistochemical analyses of desmin and junctional complex–associated proteins in control heart and desmin-mutated cardiac tissue (Glu401Asp). Positive immunoreaction is shown in brown. Scale bar=50 μm for **A** and **B**, and 100 μm for **C**.

only Data Supplement). Differentiation was confirmed by immunofluorescence for the TNNT2 cardiac marker, which demonstrated that most cells were positive. Quantitative analysis using real-time quantitative PCR (Figure 6 and Table III in the online-only Data Supplement) showed that desmin gene expression increased

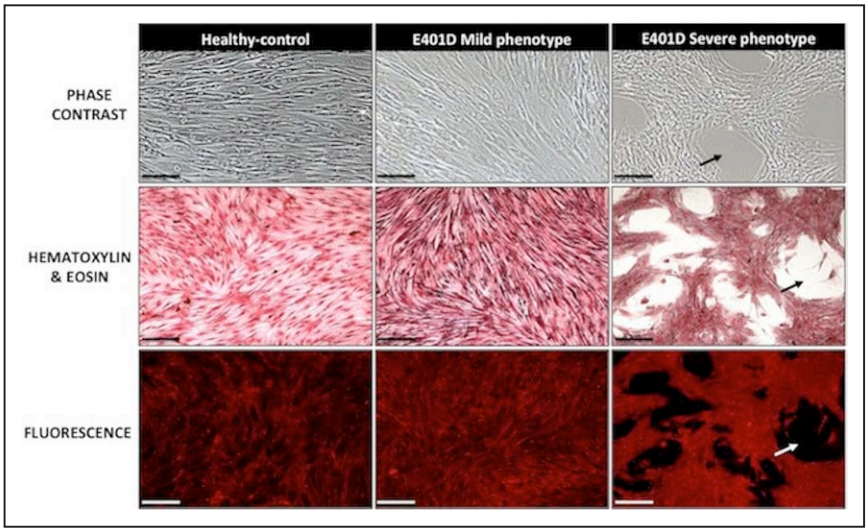

Figure 5. ADMSC differentiation analysis.
Adherence and ex vivo growth pattern of ADMSCs isolated from 3 members of the family studied, as determined by phase-contrast microscopy, hematoxylin-eosin staining, and fluorescence microscopy, showing the typical spindle-shape, elongated, and flat morphology of cells corresponding to healthy-control and mild-phenotype carrier cases and the reticular pattern shown by severe-phenotype carrier cells, with areas of the culture flask remaining uncovered by cells (arrows). Scale bar=200 µm. ADMSC indicates adipose-derived mesenchymal stem cell.

more than 23-fold in differentiated cells. However, cells carrying the *DES*-p.Glu401Asp did not show increased *DES* expression after cardiomyogenic differentiation. Analysis of the genes selected in this study showed that 9 genes were overexpressed at least 2-fold in cells from probands with mild symptomatology in comparison with healthy control samples, and 40 genes were downregulated at least 2-fold in the same samples. In turn, samples from the proband with advanced cardiomyopathy showed 11 upregulated and 37 downregulated genes in comparison with healthy controls. It is interesting to note that 4 of these genes were overexpressed and 24 downregulated in both the mild-phenotype and severe-phenotype carrier samples in comparison with healthy control samples.

Plasmids and Cell Culture

Given the effect of DES mutations on filament formation in vitro,[33] we attempted to determine whether this is also the case for the novel mutation DES-p.Glu401Asp. We used SW13 cells without any endogenous cytoplasmic intermediate filament protein expression.[34] These experiments showed that both mutations p.Glu401Asp and p.Glu401Lys, which have been previously described,[35] disrupted the intermediate filament structure in the transiently transfected cells. Both mutant desmins formed cytoplasmic aggregates, whereas wild-type desmins formed regular filaments (Figure 7).

DISCUSSION

The genes most commonly responsible for classic iARVC/D are those that encode for cardiac desmosomal proteins, being LV involvement and SCD commonly reported because of *DSP* variants.[36] Nevertheless, with the development of the advanced imaging techniques available today, we know that biventricular impairment is common, with an even worse prognosis. Also, with the advent of massive parallel sequencing techniques, nondesmosomal genes, such as *TMEM43*,[13] *TGFB3*,[37] *PLN*,[38] and *DES*,[39] whose mutations generate an iARVC/D phenotype, have been discovered. However, *DES* mutations more frequently produce a dilated or restrictive cardiomyopathy phenotype, atrioventricular conduction disorder, and skeletal myopathy.[39] This study provides strong evidence on the pathogenicity of this novel *DES* mutation as a cause of biventricular inherited arrhythmogenic cardiomyopathy/dysplasia with dominant primary LV affection, without conduction system abnormality or traces of skeletal muscular involvement. To our knowledge, this study involves the largest family of a single *DES* mutation and provides accurate genotype-phenotype cosegregation data. It is based on an interesting functional analysis that suggests the presence of a pathogenic mechanism by which desminopathy is capable of producing an iARVC/D phenotype. In addition, this mutation was not present in healthy controls and does not appear in public databases such as ClinVar or the Exome Aggregated Consortium database. Our results allow us to classify *DES* p.Glu401Asp as pathogenic according to American College of Medical Genetics and Genomics guidelines on the interpretation of genetic variants.[20]

DES mutations as a cause of iARVC/D were first described in 2009 as typically affecting the right ventricle or causing severe biventricular dysplasia.[40,41] Later, isolated cases of single mutations causing iARVC/D, which involved limited or even with no familial study, were presented.[42–44] Information on the pathogenic mechanisms of *DES* mutations to produce the inherited arrhythmogenic cardiomyopathy/dysplasia phenotype is rare. Likewise, the reasons for their cardiac and skeletal expression variability are poorly understood. Given the ability of desmin to form a network between the

Gene	Mild-Phenotype vs. Healthy-Control	Severe-Phenotype vs. Healthy-Control
ABCC9	4,32768	0,86106
ACTN1	0,36636	0,52371
ACTR1A	0,64766	0,57178
AFAP1	1,45183	0,94535
AKAP9	0,23164	0,41312
ANK2	0,38679	0,46873
ATP2A2	0,3536	0,32125
ATP2B4	0,49358	0,97577
CACNA1C	0,20212	0,2703
CACNA1D	0,06076	0,54382
CACNA1G	0,96445	0,15366
CACNA2D1	0,3289	0,30276
CACNB2	4,05873	0,15948
CALD1	0,1821	0,40811
CALM1	0,77329	0,79171
CALM2	0,31902	0,94116
CALM3	0,37843	0,78607
CAV3	0,48896	0,15495
CCNA1	0,29103	0,10184
CD36	5,49962	0,72231
DES	0,00361	0,02895
DSP	0,1792	0,73246
GAPDH	1	1
GJA1	0,0961	0,03799
GJA5	0,35027	0,10962
GPD1L	0,43803	0,56477
HAND2	0,43266	0,3182
ITGA2	2,80462	2,68293
ITGA7	0,08457	0,01089
JUP	0,07756	6,78413
KCNA5	1,12118	0,23189
KCNE1	0,42075	0,05139
KCNE1L	0,42671	0,30235
KCNE2	0,16991	0,99062
KCNE3	0,04464	1,08117
KCNH2	0,36499	0,13576
KCNJ2	3,79161	0,12035
KCNJ8	1,13837	0,46946
KRT18	0,66643	2,33748
KRT8	0,42898	0,42499
LAMA1	0,14111	0,18654
LAMA2	0,19148	0,30703
LAMA3	1,30486	25,6674
LAMA5	0,11125	0,3885
LAMB1	0,24282	0,67949
LAMB3	5,031	3,35547
LAMC2	0,50877	12,87661
LAMC3	43,35802	72,74506
LAMP2	0,3967	0,40589
LMNA	0,60073	0,83252
MST1R	0,6644	0,2444
NKX2-5	4,54454	0,26178
NPPA	1,10368	0,26172
NTN1	7,39271	4,13974
PLP1	0,60079	0,07703
PRKAG2	0,32955	0,43151
RANGRF	0,46279	0,98886
SCN1B	0,78088	3,58001
SCN3B	0,44988	0,24171
SCN4B	0,25705	0,95074
SNTA1	1,27253	1,67713
TGFB1	0,30877	1,00793
THY1	0,0618	1,164
TNF	0,87931	0,17522
TNNT2	0,01643	0,01114
TRPM4	0,70643	0,41484
TUBA1A	0,36721	1,18692
TUBA3C	0,9077	0,11774
TUBA4A	1,54778	3,58712
TUBB3	0,76403	0,30394
VIM	1,61242	5,56528

Figure 6. Quantitative gene expression analysis.
Quantitative RNA analysis heatmap revealing relative endogenous gene expression patterns after cardiomyogenic differentiation between the 2 *DES*-mutation carrier cell lines studied (mild-phenotype patient and severe-phenotype patient) and a healthy-control cell line. Colors indicate the range of each gene's expression with least expression shown in red and highest expression shown in green. For absolute quantitative values see Table III in the online-only Data Supplement.

cytoskeleton and desmosomes, the abnormal interaction between both cellular multiprotein complexes may lead to cellular adhesion defects. The desmin molecule contains 3 domains: a central α-helical rod domain flanked by 2 globular N- and C-terminal domains. The p.Glu401Asp mutation is located in segment 2B of the central rod domain, a highly conserved region in vertebrates, where most *DES* mutations were found previously.[45] Mutations at this position could eventually produce a critical break in the intra- and interhelical ionic bridges between desmin dimers, as already reported with regard to the mutation p.Glu401Lys.[35] The presence of this mutation could potentially lead to a loss of structural integrity and, consequently, of cellular adhesion, which is considered a crucial factor in the pathogenesis of iARVC/D. Our results corroborate the hypothesis of a disruption in the cellular membrane structural integrity of cells affected by mutation p.Glu401Asp. It is interesting to note that the phenotype exhibited by mutation p.Glu401Asp differs considerably from that associated with mutation p.Glu401Lys, which was described in a 20-year-old man with advanced atrioventricular block and skeletal myopathy.[35] This suggests that aspartic acid in position 401 is likely involved in the specific development of the ARVC/D phenotype with no conduction or skeletal muscle system involvement.

The histological study of the explanted heart of subject III.21 reveals affected (fibrofatty tissue replacement) and more preserved myocardial zones. It is interesting to note that, in the most preserved areas, cardiomyocytes showed an abnormal organization of their contractile apparatus, which was less abundant and poorly organized than in the control myocardium. Furthermore, the immunohistochemical study showed lower expression of desmoplakin and plakoglobin in cell junctions and did not detect any differences in connexin 43, as described elsewhere.[46] The interaction between the rod region and tail of desmin, which contain recognition binding sites implicated in the interaction with desmoplakin at the desmosome, has been previously described.[47] This means that the position of the mutation and the reduced presence of desmoplakin in the heart tissue are in line with previously published data and could be related to the increased risk of arrhythmic complications observed and to the iARVC/D phenotype. Regarding the slight decrease of plakoglobin in the intercalated disc, it could be supported by previous studies, where a decrease of plakoglobin immunoreaction is considered a consistent feature in patients with iARVC/D.[48] Surprisingly, in our study, we did not observe desmin cytoplasmic aggregates in the cardiac tissue of heterozygous carrier III.21, which appeared in transfected cells in vitro. It is well known that most of the desmin mutations are characterized by desmin-positive sarcoplasmic aggregates.[17,49] However, it was

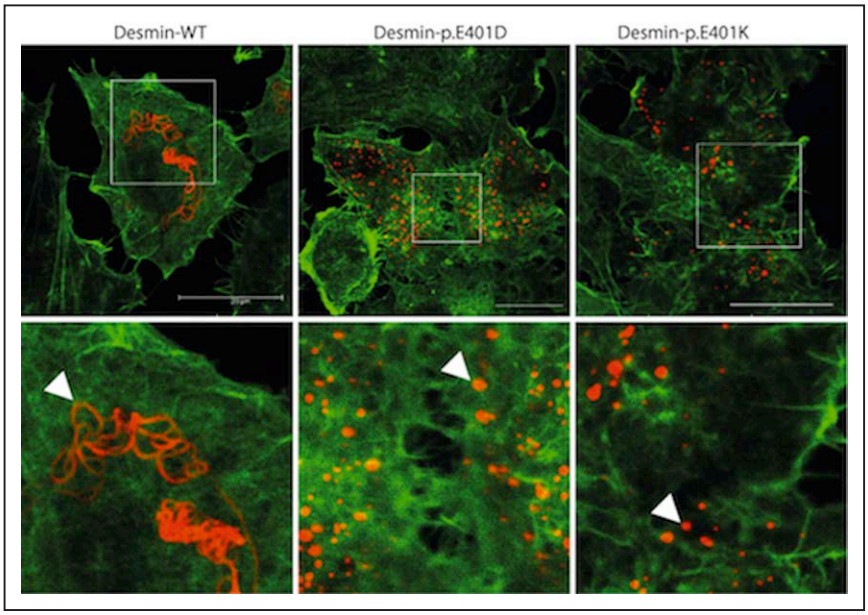

Figure 7. Desmin localization in transfected SW13 cells.
It is worth noting that the *DES* mutation p.Glu401Asp and the previously described mutation p.Glu401Lys form cytoplasmic aggregates (white arrows), whereas wild-type (WT) desmin forms intermediate filaments of different size and shape. Green, fluorescein isothiocyanate–phalloidin; red, desmin; scale bars=20 μm.

demonstrated that desmin mutations (for example, the c.1289-2A>G mutation) can manifest without the formation of these aggregates.[17,50] In our case, this absence could be related to the patient's heterozygous condition. Furthermore, we used a strong cytomegalovirus promoter in vitro, which may provoke misfolding of the mutant desmin in cell cultures. In addition, the patient's disease stage could be characterized by Z-disc disorganization and disruption of the intermediate filament network, but, with no desmin aggregates, may also explain the discrepancy of in vivo and cell culture findings of this study.[47] Finally, it is probable that this novel *DES* p.Glu401Asp mutation does not result in the formation of desmin aggregates, but its pathogenic mechanism could be related to an impairment of the adequate myofibril formation and 3-dimensional organization in the sarcoplasm. However, future studies are needed to elucidate the pathogenic mechanism related to this novel desmin mutation.

Analysis of ADMSC cultures revealed early differences between control, mild, and severe phenotypes, with striking cellular growth and adhesion defects in the patient with the severe phenotype. Following its differentiation into cardiomyocytes, RNA analysis showed that desmin expression was lower in the severe phenotype carrier. In addition, significant differences were detected in the RNA expression of different genes associated with cardiomyopathies or channelopathies. It is noteworthy that the lower RNA expression levels of a wide variety of potassium channels in both carrier groups, and the higher expression of *SCNIB*, a sodium channel with great arrhythmic potential, as well, were found. We also detected differences in the RNA expression of certain proteins between the mild and severe phenotype carriers (Figure 6 and Table III in the online-only Data Supplement). This could explain the variable clinical penetrance of iARVC/D observed in this family. These findings must be interpreted with caution, because their influence in vivo on the development of the disease remains unknown. In addition, RNA levels do not necessarily correspond to those of functional proteins in the myocardium. Incomplete clinical penetrance observed in this family is a common feature of iARVC/D. Although genetic, epigenetic, and environmental factors have been proposed, the origin of the incomplete penetrance observed in this family mentioned above is still unclear. Recent data suggest that a specific genetic background can lead to an increased susceptibility to myocarditis as part of an active phase of the disease. In our study, we did not find any myocarditis-like presentation, or suggestive data from histological analysis. However, we cannot definitely discard this possibility in this case. Future investigations are needed to address this issue.[51] It has even been suggested that sex could play a role, because the disease is usually more severe in males.[52] This was also found in the case of the family described in our study; the 4 SCD events and the 2 cardiac transplants occurred in men and, as Figure 3 shows, at an earlier age in males than in females, something described not only for p.Glu401Asp but also for other *DES* mutations.[53,54] According to our data, cardiac events in p.Glu401Asp carriers are particularly prevalent in men from 20 to 40 years, especially SCD, and life-saving therapies such as cardiac defibrillators should be promptly indicated in these cases.

In conclusion, *DES* mutation p.Glu401Asp causes iARVC/D with predominant LV involvement in the absence of skeletal myopathy and conduction system disturbance, with a high incidence of adverse clinical events. The pathogenic mechanism likely corresponds to alterations in desmin dimer assembly and its con-

nection with membrane proteins that disrupt the membrane and cell–cell adhesion integrity.

ARTICLE INFORMATION

Received April 3, 2017; accepted November 9, 2017.

The online-only Data Supplement is available with this article at http://circ.ahajournals.org/lookup/suppl/doi:10.1161/CIRCULATIONAHA.117.028719/-/DC1.

Correspondence

Francisco José Bermúdez-Jiménez, MD, Department of Cardiology, Virgen de las Nieves University Hospital, Avda Fuerzas Armadas, n2, CP: 18012, Granada, Spain. E-mail bermudezfrancisco23y@gmail.com

Affiliations

Cardiology Department, Virgen de las Nieves University Hospital, Granada, Spain (F.J.B.-J., B.A.A., M. Álvarez, S.L.-F., L.T., J.J.-J.). Department of Histology, Tissue Engineering Group, Faculty of Medicine, University of Granada, Spain (F.J.B.-J., B.A.A., M. Álvarez, S.L.-F, L.T., J.J.-J., V.C., M. Alaminos, A.C.). Instituto de Investigación Biosanitaria (F.J.B.-J., B.A.A., M. Álvarez, S.L.-F, L.T., J.J.-J., V.C., M. Alaminos, A.C.). Erich and Hanna Klessmann Institute for Cardiovascular Research and Development, Heart and Diabetes Centre North Rhine-Westphalia, Ruhr University Bochum, Bad Oeynhausen, Germany (A.B., I.S., H.M.). Cardiology Department, Health in Code, A Coruña, Spain (D.G.-G., L.M.).

Acknowledgments

The authors wish to thank Drs Rosa Ortega and Salvador Arias-Santiago for collecting tissue from the explanted heart and the adipose biopsies, respectively, for research purposes, and Laura Cortiñas for her assistance in image collecting. These results are from Dr Bermudez-Jiménez's PhD program.

Sources of Funding

Dr Milting was funded by grants from the German Research Foundation (MI 1146/2-1) and the Erich and Hanna Klessmann Foundation (Gütersloh, Germany). Histological, histochemical, immunohistochemical, real-time quantitative reverse transcription PCR, and mesenchymal stem cells differentiation studies were performed and supported by members of the Tissue Engineering Group of the Department of Histology of the University of Granada, Spain (Drs Carriel, Alaminos, and Campos).

Disclosures

None.

REFERENCES

1. Corrado D, Basso C, Thiene G, McKenna WJ, Davies MJ, Fontaliran F, Nava A, Silvestri F, Blomstrom-Lundqvist C, Wlodarska EK, Fontaine G, Camerini F. Spectrum of clinicopathologic manifestations of arrhythmogenic right ventricular cardiomyopathy/dysplasia: a multicenter study. *J Am Coll Cardiol*. 1997;30:1512–1520.
2. Marcus FI, Fontaine GH, Guiraudon G, Frank R, Laurenceau JL, Malergue C, Grosgogeat Y. Right ventricular dysplasia: a report of 24 adult cases. *Circulation*. 1982;65:384–398.
3. Sen-Chowdhry S, Syrris P, Ward D, Asimaki A, Sevdalis E, McKenna WJ. Clinical and genetic characterization of families with arrhythmogenic right ventricular dysplasia/cardiomyopathy provides novel insights into patterns of disease expression. *Circulation*. 2007;115:1710–1720. doi: 10.1161/CIRCULATIONAHA.106.660241.
4. Basso C, Corrado D, Bauce B, Thiene G. Arrhythmogenic right ventricular cardiomyopathy. *Circ Arrhythm Electrophysiol*. 2012;5:1233–1246. doi: 10.1161/CIRCEP.111.962035.
5. Corrado D, Basso C, Schiavon M, Thiene G. Screening for hypertrophic cardiomyopathy in young athletes. *N Engl J Med*. 1998;339:364–369. doi: 10.1056/NEJM199808063390602.
6. Nava A, Thiene G, Canciani B, Scognamiglio R, Daliento L, Buja G, Martini B, Stritoni P, Fasoli G. Familial occurrence of right ventricular dysplasia: a study involving nine families. *J Am Coll Cardiol*. 1988;12:1222–1228.
7. Michalodimitrakis M, Papadomanolakis A, Stiakakis J, Kanaki K. Left side right ventricular cardiomyopathy. *Med Sci Law*. 2002;42:313–317. doi: 10.1177/002580240204200406.
8. Berte B, Denis A, Amraoui S, Yamashita S, Komatsu Y, Pillois X, Sacher F, Mahida S, Wielandts JY, Sellal JM, Frontera A, Al Jefairi N, Derval N, Montaudon M, Laurent F, Hocini M, Haïssaguerre M, Jaïs P, Cochet H. Characterization of the left-sided substrate in arrhythmogenic right ventricular cardiomyopathy. *Circ Arrhythm Electrophysiol*. 2015;8:1403–1412. doi: 10.1161/CIRCEP.115.003213.
9. Sen-Chowdhry S, Syrris P, Prasad SK, Hughes SE, Merrifield R, Ward D, Pennell DJ, McKenna WJ. Left-dominant arrhythmogenic cardiomyopathy: an under-recognized clinical entity. *J Am Coll Cardiol*. 2008;52:2175–2187. doi: 10.1016/j.jacc.2008.09.019.
10. Schuler PK, Haegeli LM, Saguner AM, Wolber T, Tanner FC, Jenni R, Corti N, Lüscher TF, Brunckhorst C, Duru F. Predictors of appropriate ICD therapy in patients with arrhythmogenic right ventricular cardiomyopathy: long term experience of a tertiary care center. *PLoS One*. 2012;7:e39584.
11. Yu J, Hu J, Dai X, Cao Q, Xiong Q, Liu X, Liu X, Shen Y, Chen Q, Hua W, Hong K. SCN5A mutation in Chinese patients with arrhythmogenic right ventricular dysplasia. *Herz*. 2014;39:271–275. doi:10.1007/s00059-013-3998-5.
12. van der Zwaag PA, van Rijsingen IA, Asimaki A, Jongbloed JD, van Veldhuisen DJ, Wiesfeld AC, Cox MG, van Lochem LT, de Boer RA, Hofstra RM, Christiaans I, van Spaendonck-Zwarts KY, Lekanne dit Deprez RH, Judge DP, Calkins H, Suurmeijer AJ, Hauer RN, Saffitz JE, Wilde AA, van den Berg MP, van Tintelen JP. Phospholamban R14del mutation in patients diagnosed with dilated cardiomyopathy or arrhythmogenic right ventricular cardiomyopathy: evidence supporting the concept of arrhythmogenic cardiomyopathy. *Eur J Heart Fail*. 2012;14:1199–1207. doi: 10.1093/eurjhf/hfs119.
13. Merner ND, Hodgkinson KA, Haywood AF, Connors S, French VM, Drenckhahn JD, Kupprion C, Ramadanova K, Thierfelder L, McKenna W, Gallagher B, Morris-Larkin L, Bassett AS, Parfrey PS, Young TL. Arrhythmogenic right ventricular cardiomyopathy type 5 is a fully penetrant, lethal arrhythmic disorder caused by a missense mutation in the TMEM43 gene. *Am J Hum Genet*. 2008;82:809–821. doi: 10.1016/j.ajhg.2008.01.010.
14. Milting H, Klauke B, Christensen AH, Müsebeck J, Walhorn V, Grannemann S, Münnich T, Šarić T, Rasmussen TB, Jensen HK, Mogensen J, Baecker C, Romaker E, Laser KT, zu Knyphausen E, Kassner A, Gummert J, Judge DP, Connors S, Hodgkinson K, Young TL, van der Zwaag PA, van Tintelen JP, Anselmetti D. The TMEM43 Newfoundland mutation p.S358L causing ARVC-5 was imported from Europe and increases the stiffness of the cell nucleus. *Eur Heart J*. 2015;36:872–881. doi: 10.1093/eurheartj/ehu077.
15. Ortiz-Genga MF, Cuenca S, Dal Ferro M, Zorio E, Salgado-Aranda R, Climent V, Padrón-Barthe L, Duro-Aguado I, Jiménez-Jáimez J, Hidalgo-Olivares VM, García-Campo E, Lanzillo C, Suárez-Mier MP, Yonath H, Marcos-Alonso S, Ochoa JP, Santomé JL, García-Giustiniani D, Rodríguez-Garrido JL, Domínguez F, Merlo M, Palomino J, Peña ML, Trujillo JP, Martín-Vila A, Stolfo D, Molina P, Lara-Pezzi E, Calvo-Iglesias FE, Nof E, Calò L, Barriales-Villa R, Gimeno-Blanes JR, Arad M, García-Pavía P, Monserrat L. Truncating FLNC mutations are associated with high-risk dilated and arrhythmogenic cardiomyopathies. *J Am Coll Cardiol*. 2016;68:2440–2451. doi: 10.1016/j.jacc.2016.09.927.
16. Sarantitis I, Papanastasopoulos P, Manousi M, Baikoussis NG, Apostolakis E. The cytoskeleton of the cardiac muscle cell. *Hellenic J Cardiol*. 2012;53:367–379.
17. Capetanaki Y, Papathanasiou S, Diokmetzidou A, Vatsellas G, Tsikitis M. Desmin related disease: a matter of cell survival failure. *Curr Opin Cell Biol*. 2015;32:113–120. doi: 10.1016/j.ceb.2015.01.004.
18. Lang RM, Badano LP, Mor-Avi V, Afilalo J, Armstrong A, Ernande L, Flachskampf FA, Foster E, Goldstein SA, Kuznetsova T, Lancellotti P, Muraru D, Picard MH, Rietzschel ER, Rudski L, Spencer KT, Tsang W, Voigt JU. Recommendations for cardiac chamber quantification by echocardiography in adults: an update from the American Society of Echocardiography and the European Association of Cardiovascular Imaging. *Eur Heart J Cardiovasc Imaging*. 2015;16:233–270. doi: 10.1093/ehjci/jev014.
19. Marcus FI, McKenna WJ, Sherrill D, Basso C, Bauce B, Bluemke DA, Calkins H, Corrado D, Cox MG, Daubert JP, Fontaine G, Gear K, Hauer R, Nava A, Picard MH, Protonotarios N, Saffitz JE, Sanborn DM, Steinberg JS, Tandri H, Thiene G, Towbin JA, Tsatsopoulou A, Wichter T, Zareba W. Diagnosis of arrhythmogenic right ventricular cardiomyopathy/dysplasia: proposed

modification of the Task Force Criteria. *Eur Heart J*. 2010;31:806–814. doi: 10.1093/eurheartj/ehq025.
20. Richards S, Aziz N, Bale S, Bick D, Das S, Gastier-Foster J, Grody WW, Hegde M, Lyon E, Spector E, Voelkerding K, Rehm HL; ACMG Laboratory Quality Assurance Committee. Standards and guidelines for the interpretation of sequence variants: a joint consensus recommendation of the American College of Medical Genetics and Genomics and the Association for Molecular Pathology. *Genet Med*. 2015;17:405–424. doi: 10.1038/gim.2015.30.
21. Carriel V, Campos F, Aneiros-Fernández J, Kiernan JA. Tissue fixation and processing for the histological identification of lipids. *Methods Mol Biol*. 2017;1560:197–206. doi:10.1007/978-1-4939-6788-9_14.
22. Carriel V, Aneiros-Fernández J, Ruyffelaert M, Arias-Santiago S, Riady V, Izquierdo-Martínez F, Roda O, Cornelissen M, Campos A, Alaminos M. Histological and immunohistochemical study of an unusual type of gallbladder duplication. *Histol Histopathol*. 2014;29:957–964. doi: 10.14670/HH-29.957.
23. Kiernan JA. *Histological and Histochemical Methods: Theory and Practice*. 3rd ed. Boston, MA: Butterworth Heinemann; 1999.
24. Carriel V, Garzón I, Campos A, Cornelissen M, Alaminos M. Differential expression of GAP-43 and neurofilament during peripheral nerve regeneration through bio-artificial conduits. *J Tissue Eng Regen Med*. 2017;11:553–563. doi: 10.1002/term.1949.
25. Brodehl A, Dieding M, Biere N, Unger A, Klauke B, Walhorn V, Gummert J, Schulz U, Linke WA, Gerull B, Vorgert M, Anselmetti D, Milting H. Functional characterization of the novel DES mutation p.L136P associated with dilated cardiomyopathy reveals a dominant filament assembly defect. *J Mol Cell Cardiol*. 2016;91:207–214. doi: 10.1016/j.yjmcc.2015.12.015.
26. Stenson PD, Ball EV, Mort M, Phillips AD, Shiel JA, Thomas NS, Abeysinghe S, Krawczak M, Cooper DN. Human Gene Mutation Database (HGMD): 2003 update. *Hum Mutat*. 2003;21:577–581. doi: 10.1002/humu.10212.
27. Sherry ST, Ward MH, Kholodov M, Baker J, Phan L, Smigielski EM, Sirotkin K. dbSNP: the NCBI database of genetic variation. *Nucleic Acids Res*. 2001;29:308–311.
28. Fu W, O'Connor TD, Jun G, Kang HM, Abecasis G, Leal SM, Gabriel S, Rieder MJ, Altshuler D, Shendure J, Nickerson DA, Bamshad MJ, Akey JM; NHLBI Exome Sequencing Project. Analysis of 6,515 exomes reveals the recent origin of most human protein-coding variants. *Nature*. 2013;493:216–220. doi: 10.1038/nature11690.
29. Landrum MJ, Lee JM, Benson M, Brown G, Chao C, Chitipiralla S, Gu B, Hart J, Hoffman D, Hoover J, Jang W, Katz K, Ovetsky M, Riley G, Sethi A, Tully R, Villamarin-Salomon R, Rubinstein W, Maglott DR. ClinVar: public archive of interpretations of clinically relevant variants. *Nucleic Acids Res*. 2016;44(D1):D862–D868. doi: 10.1093/nar/gkv1222.
30. Lek M, Karczewski KJ, Minikel EV, Samocha KE, Banks E, Fennell T, O'Donnell-Luria AH, Ware JS, Hill AJ, Cummings BB, Tukiainen T, Birnbaum DP, Kosmicki JA, Duncan LE, Estrada K, Zhao F, Zou J, Pierce-Hoffman E, Berghout J, Cooper DN, Deflaux N, DePristo M, Do R, Flannick J, Fromer M, Gauthier L, Goldstein J, Gupta N, Howrigan D, Kiezun A, Kurki MI, Moonshine AL, Natarajan P, Orozco L, Peloso GM, Poplin R, Rivas MA, Ruano-Rubio V, Rose SA, Ruderfer DM, Shakir K, Stenson PD, Stevens C, Thomas BP, Tiao G, Tusie-Luna MT, Weisburd B, Won HH, Yu D, Altshuler DM, Ardissino D, Boehnke M, Danesh J, Donnelly S, Elosua R, Florez JC, Gabriel SB, Getz G, Glatt SJ, Hultman CM, Kathiresan S, Laakso M, McCarroll S, McCarthy MI, McGovern D, McPherson R, Neale BM, Palotie A, Purcell SM, Saleheen D, Scharf JM, Sklar P, Sullivan PF, Tuomilehto J, Tsuang MT, Watkins HC, Wilson JG, Daly MJ, MacArthur DG; Exome Aggregation Consortium. Analysis of protein-coding genetic variation in 60,706 humans. *Nature*. 2016;536:285–291. doi: 10.1038/nature19057.
31. Kim C, Wong J, Wen J, Wang S, Wang C, Spiering S, Kan NG, Forcales S, Puri PL, Leone TC, Marine JE, Calkins H, Kelly DP, Judge DP, Chen HS. Studying arrhythmogenic right ventricular dysplasia with patient-specific iPSCs. *Nature*. 2013;494:105–110. doi: 10.1038/nature11799.
32. Brodehl A, Dieding M, Klauke B, Dec E, Madaan S, Huang T, Gargus J, Fatima A, Saric T, Cakar H, Walhorn V, Tönsing K, Skrzipczyk T, Cebulla R, Gerdes D, Schulz U, Gummert J, Svendsen JH, Olesen MS, Anselmetti D, Christensen AH, Kimonis V, Milting H. The novel desmin mutant p.A120D impairs filament formation, prevents intercalated disk localization, and causes sudden cardiac death. *Circ Cardiovasc Genet*. 2013;6:615–623. doi: 10.1161/CIRCGENETICS.113.000103.
33. Brodehl A, Hedde PN, Dieding M, Fatima A, Walhorn V, Gayda S, Šarić T, Klauke B, Gummert J, Anselmetti D, Heilemann M, Nienhaus GU, Milting H. Dual color photoactivation localization microscopy of cardiomyopathy-associated desmin mutants. *J Biol Chem*. 2012;287:16047–16057. doi: 10.1074/jbc.M111.313841.
34. Hescheler J, Meyer R, Plant S, Krautwurst D, Rosenthal W, Schultz G. Morphological, biochemical, and electrophysiological characterization of a clonal cell (H9c2) line from rat heart. *Circ Res*. 1991;69:1476–1486.
35. Goudeau B, Rodrigues-Lima F, Fischer D, Casteras-Simon M, Sambuughin N, de Visser M, Laforet P, Ferrer X, Chapon F, Sjöberg G, Kostareva A, Sejersen T, Dalakas MC, Goldfarb LG, Vicart P. Variable pathogenic potentials of mutations located in the desmin alpha-helical domain. *Hum Mutat*. 2006;27:906–913. doi: 10.1002/humu.20351.
36. Bauce B, Basso C, Rampazzo A, Beffagna G, Daliento L, Frigo G, Malacrida S, Settimo L, Danieli G, Thiene G, Nava A. Clinical profile of four families with arrhythmogenic right ventricular cardiomyopathy caused by dominant desmoplakin mutations. *Eur Heart J*. 2005;26:1666–1675. doi: 10.1093/eurheartj/ehi341.
37. Beffagna G, Occhi G, Nava A, Vitiello L, Ditadi A, Basso C, Bauce B, Carraro G, Thiene G, Towbin JA, Danieli GA, Rampazzo A. Regulatory mutations in transforming growth factor-beta3 gene cause arrhythmogenic right ventricular cardiomyopathy type 1. *Cardiovasc Res*. 2005;65:366–373. doi: 10.1016/j.cardiores.2004.10.005.
38. Groeneweg JA, van der Zwaag PA, Jongbloed JD, Cox MG, Vreeker A, de Boer RA, van der Heijden JF, van Veen TA, McKenna WJ, van Tintelen JP, Dooijes D, Hauer RN. Left-dominant arrhythmogenic cardiomyopathy in a large family: associated desmosomal or nondesmosomal genotype? *Heart Rhythm*. 2013;10:548–559. doi: 10.1016/j.hrthm.2012.12.020.
39. Taylor MR, Slavov D, Ku L, Di Lenarda A, Sinagra G, Carniel E, Haubold K, Boucek MM, Ferguson D, Graw SL, Zhu X, Cavanaugh J, Sucharov CC, Long CS, Bristow MR, Lavori P, Mestroni L; Familial Cardiomyopathy Registry; BEST (Beta-Blocker Evaluation of Survival Trial) DNA Bank. Prevalence of desmin mutations in dilated cardiomyopathy. *Circulation*. 2007;115:1244–1251. doi: 10.1161/CIRCULATIONAHA.106.646778.
40. van Tintelen JP, Van Gelder IC, Asimaki A, Suurmeijer AJ, Wiesfeld AC, Jongbloed JD, van den Wijngaard A, Kuks JB, van Spaendonck-Zwarts KY, Notermans N, Boven L, van den Heuvel F, Veenstra-Knol HE, Saffitz JE, Hofstra RM, van den Berg MP. Severe cardiac phenotype with right ventricular predominance in a large cohort of patients with a single missense mutation in the DES gene. *Heart Rhythm*. 2009;6:1574–1583. doi: 10.1016/j.hrthm.2009.07.041.
41. Otten E, Asimaki A, Maass A, van Langen IM, van der Wal A, de Jonge N, van den Berg MP, Saffitz JE, Wilde AA, Jongbloed JD, van Tintelen JP. Desmin mutations as a cause of right ventricular heart failure affect the intercalated disks. *Heart Rhythm*. 2010;7:1058–1064. doi: 10.1016/j.hrthm.2010.04.023.
42. Klauke B, Kossmann S, Gaertner A, Brand K, Stork I, Brodehl A, Dieding M, Walhorn V, Anselmetti D, Gerdes D, Bohms B, Schulz U, Zu Knyphausen E, Vorgerd M, Gummert J, Milting H. De novo desmin-mutation N116S is associated with arrhythmogenic right ventricular cardiomyopathy. *Hum Mol Genet*. 2010;19:4595–4607. doi: 10.1093/hmg/ddq387.
43. Lorenzon A, Beffagna G, Bauce B, De Bortoli M, Li Mura IE, Calore M, Dazzo E, Basso C, Nava A, Thiene G, Rampazzo A. Desmin mutations and arrhythmogenic right ventricular cardiomyopathy. *Am J Cardiol*. 2013;111:400–405. doi: 10.1016/j.amjcard.2012.10.017.
44. Ripoll-Vera T, Zorio E, Gámez JM, Molina P, Govea N, Crémer D. Phenotypic patterns of cardiomyopathy caused by mutations in the desmin gene. a clinical and genetic study in two inherited heart disease units. *Rev Esp Cardiol (Engl Ed)*. 2015;68:1027–1029.
45. Azzimato V, Gennebäck N, Tabish AM, Buyandelger B, Knöll R. Desmin, desminopathy and the complexity of genetics. *J Mol Cell Cardiol*. 2017;92:93–95. doi:10.1016/j.yjmcc.2016.01.017.
46. Goldfarb LG, Dalakas MC. Tragedy in a heartbeat: malfunctioning desmin causes skeletal and cardiac muscle disease. *J Clin Invest*. 2009;119:1806–1813. doi: 10.1172/JCI38027.
47. Lapouge K, Fontao L, Champliaud MF, Jaunin F, Frias MA, Favre B, Paulin D, Green KJ, Borradori L. New insights into the molecular basis of desmoplakin- and desmin-related cardiomyopathies. *J Cell Sci*. 2006;119(pt 23):4974–4985. doi: 10.1242/jcs.03255.
48. Asimaki A, Tandri H, Huang H, Halushka MK, Gautam S, Basso C, Thiene G, Tsatsopoulou A, Protonotarios N, McKenna WJ, Calkins H, Saffitz JE. A new diagnostic test for arrhythmogenic right ventricular cardiomyopathy. *N Engl J Med*. 2009;360:1075–1084. doi: 10.1056/NEJMoa0808138.
49. Smolina N, Bruton J, Sjoberg G, Kostareva A, Sejersen T. Aggregate-prone desmin mutations impair mitochondrial calcium uptake in primary myotubes. *Cell Calcium*. 2014;56:269–275. doi: 10.1016/j.ceca.2014.08.001.

50. Cetin N, Balci-Hayta B, Gundesli H, Korkusuz P, Purali N, Talim B, Tan E, Selcen D, Erdem-Ozdamar S, Dincer P. A novel desmin mutation leading to autosomal recessive limb-girdle muscular dystrophy: distinct histopathological outcomes compared with desminopathies. *J Med Genet*. 2013;50:437–443. doi: 10.1136/jmedgenet-2012-101487.
51. Lopez-Ayala JM, Pastor-Quirante F, Gonzalez-Carrillo J, Lopez-Cuenca D, Sanchez-Munoz JJ, Oliva-Sandoval MJ, Gimeno JR. Genetics of myocarditis in arrhythmogenic right ventricular dysplasia. *Heart Rhythm*. 2015;12:766–773. doi: 10.1016/j.hrthm.2015.01.001.
52. Mazzanti A, Ng K, Faragli A, Maragna R, Chiodaroli E, Orphanou N, Monteforte N, Memmi M, Gambelli P, Novelli V, Bloise R, Catalano O, Moro G, Tibollo V, Morini M, Bellazzi R, Napolitano C, Bagnardi V, Priori SG. Arrhythmogenic right ventricular cardiomyopathy: clinical course and predictors of arrhythmic risk. *J Am Coll Cardiol*. 2016;68:2540–2550. doi: 10.1016/j.jacc.2016.09.951.
53. Li D, Tapscoft T, Gonzalez O, Burch PE, Quiñones MA, Zoghbi WA, Hill R, Bachinski LL, Mann DL, Roberts R. Desmin mutation responsible for idiopathic dilated cardiomyopathy. *Circulation*. 1999;100:461–464.
54. Bär H, Schopferer M, Sharma S, Hochstein B, Mücke N, Herrmann H, Willenbacher N. Mutations in desmin's carboxy-terminal "tail" domain severely modify filament and network mechanics. *J Mol Biol*. 2010;397:1188–1198. doi: 10.1016/j.jmb.2010.02.024.